ESR study of the structure and production of $Sn^-(5p^3,^4S)$ defects in alkali halides

Frank Van Steen and Dirk Schoemaker
Physics Department, University of Antwerp (U.I.A.), B-2610 Wilrijk, Belgium
(Received 5 July 1978)

Several complex Sn^- defects are produced in KCl:Sn^{2+} by x irradiation, followed by suitable thermal and optical treatments. The $Sn^-(5p^3,^4S)$ ions which occupy anion sites are identified by their characteristic $S = 3/2$ ESR spectra exhibiting dominant zero-field splittings. In the Sn^-(cubic) center the Sn^- occupies an unperturbed anion site. The Sn^-(tetrag) defect has tetragonal symmetry around ⟨100⟩, and the Sn^- is associated with either a cation vacancy or a cation-anion divacancy along ⟨100⟩. The z axes of the orthorombic defects Sn^-(ortho,1) and Sn^-(ortho,2) make small angles, 2.1° and 1.4°, respectively, with the ⟨110⟩ directions in the {100} planes. Each of these two defects must be associated with at least two vacancies, inducing a dominant tetragonal field component nearly along ⟨110⟩. Production, pulse-anneal, and selective optical F- and V_K-center bleaching experiments are performed in order to try to establish the production mechanism of these complex Sn^- defects, in particular the change to a negative-ion position of the tin. These experiments indicate that the production proceeds via the high-temperature Sn^+ defects and via a defect consisting of a Sn^0 atom occupying an anion-cation vacancy pair. Subsequent trapping of an electron and of vacancies results in the formation of the complex Sn^- defects.

I. INTRODUCTION

The ns^2 heavy-metal ion impurities (Tl^+, Pb^{2+}, Sn^{2+}, In^+, Ga^+, etc....) in the alkali halides have been the subject of many investigations. On the one hand, the optical-absorption and luminescence properties, largely determined by the excited $nsnp$ configuration, have received considerable attention because the latter is a model system for the study of the Jahn-Teller effect.[1] On the other hand, these ions are good traps for both electrons and positive holes produced by ionizing radiation at low temperatures. Hole trapping results in the $ns^1(^2S)$ species, such as Tl^{2+}, Pb^{3+}, and Sn^{3+} whose ESR and optical spectra are readily detected.[2-5] Electron trapping results in the formation of, e.g., Tl^0, Pb^+, and Sn^+ defects, but only for the latter ion have the ESR spectra been detected and studied together with the optical-absorption properties.[6] There is no doubt, however, from, e.g., optical-absorption work[2,7] that the Tl^0 and Pb^+ species exist, but their ESR spectra have never been observed even after careful searches.

A continued study of the electron-trapping properties of these heavy-metal ion impurities has recently yielded complex new defects. For example, Tl^0- and Pb^+-type defects related to, but different from, the long-sought-after Tl^0 and Pb^+ centers have been observed in ESR.[8] KCl:Sn^{2+} turned out to be a particularly complex and fruitful system for investigation,[9] and the results of an ESR study are presented in this paper. It will be shown that Sn^{2+} can trap several electrons and exchange lattice sites under x irradiation with the result that complex Sn^--type defects are formed. Although the production in alkali halides of negative ions out of positive-ion impurities is not new (e.g., Au^- and Ag^- have been identified[10,11]), these studies were in general based on additively or electrolytically colored crystals, or on heavily x-irradiated crystals. Furthermore, because these defects are in general nonmagnetic, the investigations were limited mostly to employing optical techniques. The present study is the first one to use resonance techniques in the study of these types of negative-ion defects.

The structure of the paper is as follows. In Sec. III the ESR spectra of x-irradiated KCl:Sn^{2+} will be analyzed and it will be shown that one is dealing with Sn^- defects on negative-ion sites. In Sec. IV an attempt is made to present specific models for the four observed Sn^- defects drawing on the primary ESR data as well on results obtained in Secs. V–VIII. In Secs. V and VI production curves and optical and thermal data of the Sn^- defects are presented. Finally, in Sec. VII a limited attempt is presented to explain the production of the Sn^- defects by x irradiation.

II. EXPERIMENTAL

The Sn^{2+}-doped alkali halides used in these experiments were grown by the Bridgeman method and were similar to the ones used in Ref. 6. Typically 0.2-mol% $SnCl_2$ was added to the alkali-halide melt. The x rays used to produce the defects came from a Siemens tube with a tungsten target operating at 50 kV and 50 mA. Before irradiation the specimens were heated to about 350 °C for several minutes and then cooled down to room temperature or lower. For the irradiation

the specimens were placed in a groove on top of a long aluminum block and covered with a 1 mm thin plate of fused silica wrapped in thin aluminum foil. This combination acted as a filter for the soft x rays. For irradiations below room temperature, the lower part of the aluminum block was inserted in liquid N_2. The upper part had a heater coil around it. A sensor and a temperature controller permitted the regulation of the irradiation temperature to within a few degrees. The same setup was used for the pulse-anneal measurements.

For the ESR measurements a Varian E-12 spectrometer was used operating at X-band frequencies. Into the multipurpose microwave cavity an Air-Products Helitran double walled quartz Dewar was inserted permitting variable-temperature ESR measurements down to about 8 K using a heated stream of evaporating cold helium gas. The unsilvered fused silica Dewar walls and slits in the front cavity wall made possible the *in situ* optical excitation of the ESR samples down to the lowest obtainable temperatures. These optical excitations were done using a 200-W high-pressure Hg lamp in combination with appropriate Bausch and Lomb interference filters and Corning Glass cutoff filters.

The magnetic field measurements were done using an AEG-Telefunken NMR gauss meter and a HP 5248M frequency counter in combination with a digital NMR-frequency-to-magnetic-field converter.[12]

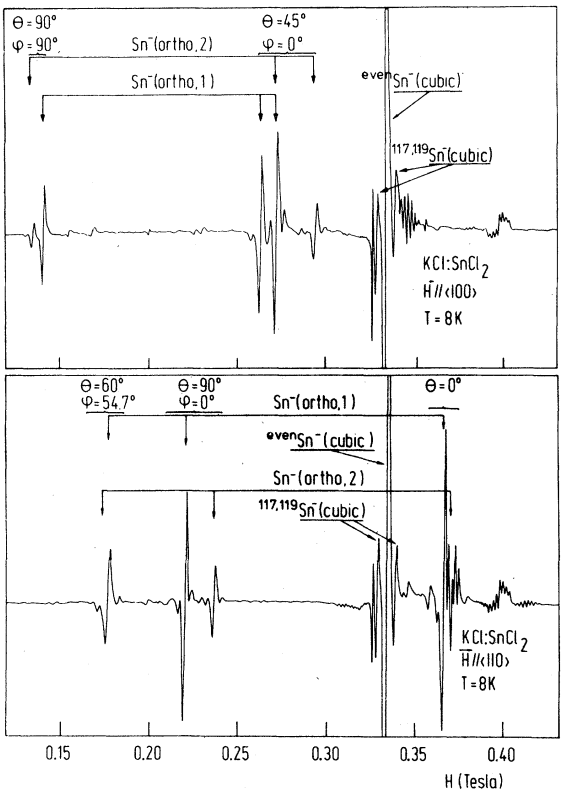

FIG. 1. ESR spectra at about 8 K of Sn^- (cubic), Sn^-(ortho, 1), and Sn^-(ortho, 2) in KCl:Sn^{2+} produced by x irradiation at room temperature. The first derivative of the absorption is presented. Microwave frequency $\nu = 9.16$ GHz.

III. ELECTRON PARAMAGNETIC RESONANCE OF Sn^-

A. Production, description, and nomenclature

Four different tin centers, which will be shown to be essentially Sn^- centers, are produced in KCl:Sn^{2+} crystals by ionizing radiation and suitable thermal and optical treatment. The first center, called Sn^- (cubic), is most readily formed by x irradiation at room temperature. Its EPR spectrum (Fig. 1) consists of a single line whose position is isotropic, flanked by two weak hyperfine (hf) satellites (weaker by a factor of 10) whose separation and position are also isotropic. The single line originates from centers involving the even tin isotopes (altogether 83.8% abundant) which possess no nuclear spin, while the two hf satellites originate from the uneven isotopes ^{117}Sn (7.51%) and ^{119}Sn (8.45%), both of which have nuclear spin $I = \frac{1}{2}$ and very nearly the same nuclear moments [$\mu_N(^{117}\text{Sn}) = -0.9951$ and $\mu_N(^{119}\text{Sn}) = -1.0411$ nuclear magnetons]. That this interpretation is correct is shown by the observation that in a KCl specimen doped with 90-at.% enriched ^{119}Sn, the two hf lines are each stronger than the single line by a factor of about 4.5, as they should be (see Fig. 2). Thus the fact that a single tin nucleus is involved in the Sn^- (cubic) center is well established.

The second center, called Sn^- (tetrag), can be produced in three different ways. The most direct way is to x irradiate a KCl:Sn^{2+} specimen at 230 K. The concentration thus obtained is rather low, but the advantage of this treatment is that no Sn^- (cubic) is produced. A much stronger EPR spectrum is produced by first x irradiating the specimen for a short time (±5 min) at room temperature, followed by a comparable irradiation at 77 K. A third method consists of either x irradiation at 200 K followed by a warm-up to room temperature or an x irradiation at room temperature, both followed by a F-center optical excitation at 10 K.

Figure 3 presents the EPR spectra for the $\vec{H} \| \langle 100 \rangle$ and $\vec{H} \| \langle 110 \rangle$ directions of the static magnetic field $\vec{H}$. The spectra are characterized by anisotropic single lines possessing axial sym-

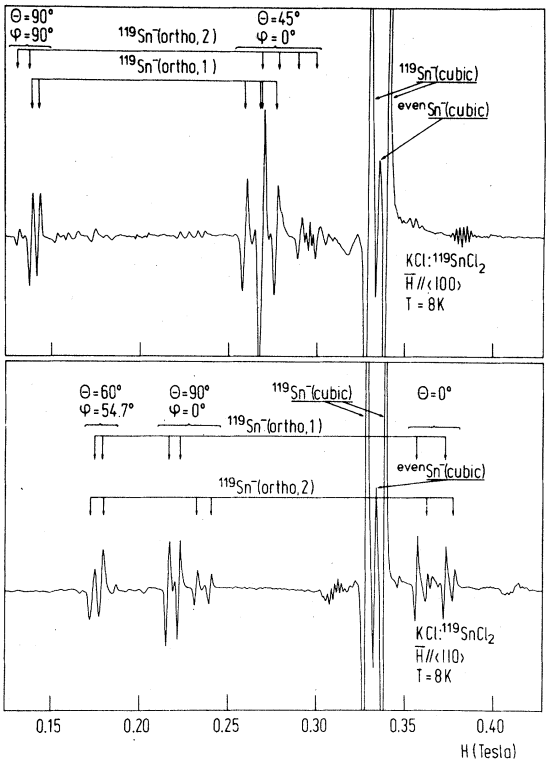

FIG. 2. Same as Fig. 1, but in a 90% enriched KCl: $^{119}Sn^{2+}$ crystal, clearly showing the ^{119}Sn doublet hyperfine splittings.

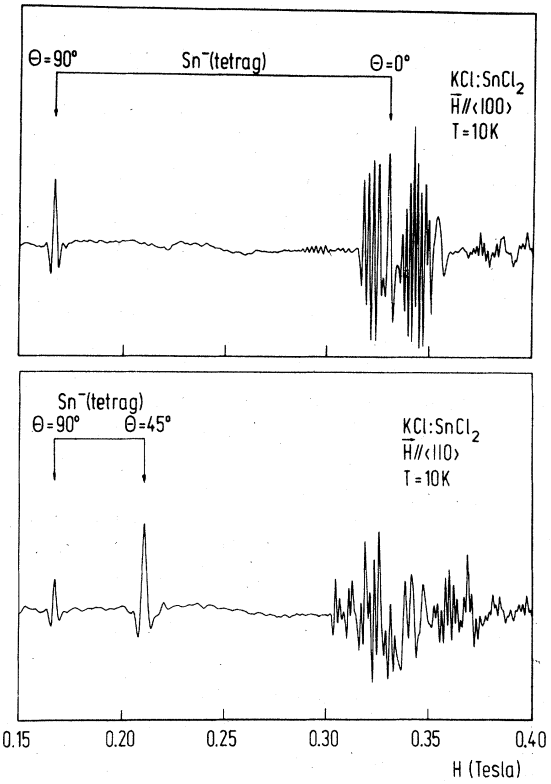

FIG. 3. ESR spectra at about 10 K of Sn^-(tetrag) in KCl:Sn^{2+} produced by x irradiation at 230 K. By this treatment no interfering Sn^-(cubic) is produced. The second derivative of the absorption is presented. Microwave frequency $\nu = 9.16$ GHz.

metry around the ⟨100⟩ directions. The single lines are accompanied by two hf satellites originating from hf interaction with single ^{117}Sn and ^{119}Sn nuclei. This is clearly proven by experiments in a KCl crystal doped with 90% ^{119}Sn; the dominant spectrum here is an anisotropic hf doublet.

The third and fourth center, called Sn^- (ortho, 1) and Sn^- (ortho, 2) are produced by an x irradiation at room temperature. The Sn^- (ortho, 1) concentration thus obtained is strong, but the Sn^- (ortho, 2) intensity is rather small. A much stronger Sn^- (ortho, 2) is realized by first x irradiating at 200 K followed by a warm-up to 285 K (see Sec. VI). Analysis of the EPR spectra (Figs. 1 and 2) shows that they both consist of anisotropic single lines or hf doublets possessing orthorhombic symmetry. For Sn^- (ortho, 1) the z axis makes a 2.1° angle with [110] in the (001) plane, and $\vec{y} \| [001]$. Sn^- (ortho, 2) possesses the same symmetry, but the tipping angle of z with ⟨110⟩ is 1.4°. This tipping of the z axis is the cause of the splitting of the $\theta = 45°$, $\varphi = 0°$ lines in Figs. 1 and 2. θ and φ are the polar angles of the external magnetic field $\vec{H}$ with respect to the symmetry axes x, y, and z of the centers. That a single tin nucleus is involved in these centers is again proven by experiments in 90% enriched ^{119}Sn-doped KCl crystals where the hf doublets are the prominent feature (Fig. 2).

The EPR linewidths of these four centers are comparable to one another and are in the range of $(15 \text{ to } 19) \times 10^{-4}$ T. Finally, there is evidence from the ESR spectra (Figs. 1 and 2) that there is at least one more Sn^- (ortho)-type center. Because of its low intensity, it was not further analyzed.

B. Analysis of EPR spectra

1. Formal analysis as $S = \frac{1}{2}$ systems

The EPR spectra of the four Sn^- centers are characterized by single lines exhibiting a doublet hf separation of small magnitude for ^{119}Sn and ^{117}Sn, but showing no fine-structure splittings. A quantitative analysis shows that the spectra can be described formally by the following simple spin Hamiltonian in which the Zeeman term is dominant (usual notation):

$$\mathcal{H}/g_0\mu_B = (1/g_0)\vec{H} \cdot \vec{g}^{\,\text{eff}} \cdot \vec{S} + \vec{S} \cdot \vec{A}^{\,\text{eff}} \cdot \vec{I} \qquad (1)$$

TABLE I. ESR results of the Sn^- (cubic), Sn^- (tetrag), Sn^- (ortho, 1), and Sn^- (ortho, 2) centers in $KCl:SnCl_2$ at ~ 10 K; (i) treated as $S = \frac{1}{2}$ systems with spin Hamiltonian (1); (ii) treated as $S = \frac{3}{2}$ systems with spin Hamiltonian (2). The linewidths ΔH and hyperfine parameters are expressed in units of 10^{-4} T.

	Center	g_z^{eff}	g_x^{eff}	g_y^{eff}	A_z^{eff}	A_x^{eff}	A_y^{eff}	Linewidth ΔH	T_{decay}
	Sn^- (cubic)		1.9700			107.7		18 ± 1	+140 °C
			±0.0005			± 0.5			
	Sn^- (tetrag) [a]	1.987	3.931		97	152		19 ± 1 [d]	−20 °C
(i)		±0.001	±0.001		± 2	± 1			
	Sn^- (ortho, 1) [b]	1.895	2.982	4.652	164	91	89	15 ± 1 [d]	+70 °C
		±0.001	±0.002	±0.002	± 1	± 2	± 2		
	Sn^- (ortho, 2) [c]	1.762	2.778	4.853	136	113	147	15 ± 1 [d]	+20 °C [e]
		±0.001	±0.002	±0.002	± 1	± 2	± 2		+70 °C

		g_z	$g_\perp$	A_z	A_x	A_y	E/D	D (cm^{-1})	ΔH	T_{decay}
	Sn^- (cubic)		1.9700		107.7		0	0	18 ± 1	+140 °C
	Sn^- (tetrag) [a]	1.986	1.965	97		76	0	•••	19 ± 1 [d]	−20 °C
(ii)		⟨1.976⟩			⟨ 83⟩					
	Sn^- (ortho, 1) [b]	2.002	1.939	161	60	37	0.14	>17	15 ± 1 [d]	+70 °C
		⟨1.954⟩			⟨ 86⟩					
	Sn^- (ortho, 2) [c]	1.948	1.952	150	79	59	0.19	•••	15 ± 1 [d]	+20 °C [e]
		⟨1.950⟩			⟨ 96⟩					+70 °C

[a] For Sn^- (tetrag): $\vec{z} \| \langle 100 \rangle$.
[b] For Sn^- (ortho, 1): $\vec{z} \| \{[110] + 2.1°$ in $(001)\}$, $\vec{y} \| [001]$.
[c] For Sn (ortho, 2): $\vec{z} \| \{[110] + 1.4°$ in $(001)\}$, $\vec{y} \| [001]$.
[d] $\theta = 0°$ linewidth.
[e] This is not the true decay temperature of Sn^- (ortho, 2): see Figs. 13 and 14.

with $S = \frac{1}{2}$ and $I = \frac{1}{2}$, and in which the main axes of the $\vec{g}^{eff}$ and $\vec{A}^{eff}$ tensors coincide. Fitting the EPR spectra to (1) results in the parameters as given in the upper half of Table I. A noteworthy observation is that the perpendicular g^{eff} components of the anisotropic spectra deviate very strongly from the free-electron value 2.0023. In fact for both Sn^- (tetrag) and Sn^- (ortho), $g_\perp^{eff} \approx 4$, whereas, $g_\parallel^{eff} \approx 2$.

2. Impossibility of Sn^0, Sn^+, Sn^{3+} and molecular models

Two facts may be emphasized. First, only one tin nucleus is involved in each of the four centers. This indicates that they are either atomic in character or molecular in character, but in the latter case the elements involving the remainder of the molecule should posses no nuclear spin. Second, for Sn^- (tetrag) and Sn^- (ortho) the g^{eff} values deviate very strongly from the free-spin value and this points to a paramagnetic system with sizeable degeneracy (orbital or spin) in the ground state, a degeneracy which is partly lifted by the crystal field. This eliminates all molecular models for the centers, except possibly linear molecules involving a single tin nucleus and possessing a $^2\Pi$ ground state.

However, a free linear molecule (homonuclear or heteronuclear) in a $^2\Pi$ ground state leads to $g_\parallel = 4$ and $g_\perp = 0$ values where $\parallel$ and $\perp$ correspond to parallel and perpendicular to the molecular axis.[13] In a crystal field of suitable low symmetry and sufficient strength such a molecule leads to $g_\parallel \approx g_\perp \approx 2$. The observed g^{eff} values in our case cannot be reconciled with this behavior.

We are led then to an atomic or ionic model for the four centers. Because the Sn^{2+} impurities are on a positive-ion site before irradiation, trapping of electrons or holes can then *a priori* lead to the following paramagnetic possibilities: $Sn^0(5s^25p^2, {}^3P)$, $Sn^+(5s^25p^1, {}^2P)$, and $Sn^{3+}(5s^1, {}^2S)$.

The Sn^{3+} model can be rejected because such a species has been observed.[5] It is characterized by an isotropic g factor close to 2 and a very large ($\gg$ Zeeman energy) hyperfine interaction (25 GHz). Furthermore there are resolved superhyperfine effects with six surrounding Cl^- ions. The Sn^{3+} is very similar to[4] Pb^{3+}.

The Sn^+ model must also be rejected. Indeed, such species have been studied quite thoroughly.[6] The Sn^+ g values ($g_\parallel = 1.8952, g_\perp = 1.6494$) are quite different from those in Table I, and also the Sn^+ hf interaction is very much larger ($\approx 900 \times 10^{-4}$T) than the values presented in Table I. It is hard

to see how the Sn^+ parameters could be modified so much by another environment as to yield numbers comparable to the ones obtained here. Furthermore, Sn^+ centers exhibit clearly resolved and anisotropic hf effects with surrounding Cl^- ions, which is not the case here.

The Sn^0 model must also be rejected because its $S=1$ ground state is not compatible with the fact that the spectra can be described formally as $S=\frac{1}{2}$ systems.

3. Identification as Sn^-: Analysis as an $S=3/2$ system

A way out of the difficulties is to propose another atomic model for the basic species, namely, a $Sn^-(5s^25p^3, {}^4S_{3/2})$ ion, which is characterized by a $S=\frac{3}{2}$ in the ground state. The spin degeneracy may be partially lifted by crystal fields of suitable low symmetry and the general spin Hamiltonian describing the EPR spectrum of such species has the form (usual notations):

$$\mathcal{H}/g_0\mu_B = DS_z^2 + E(S_x^2 - S_y^2) + (1/g_0)\vec{H}\cdot\vec{g}\cdot\vec{S} + \vec{S}\cdot\vec{A}\cdot\vec{I}\,, \tag{2}$$

with $S=\frac{3}{2}$ and $I=\frac{1}{2}$. This spin Hamiltonian will be solved with the assumption:

$$D > (g/g_0)H\,,$$

and this will result in two well-separated Kramers doublets each of which can be described formally as a $S=\frac{1}{2}$ system.

Although the problem can be solved exactly for $\vec{H}$ parallel to any of the three principal axes, it is much more instructive, and equally accurate in our case, to treat it in the following approximate fashion. First, the two crystal-field terms in (2) are diagonalized in the $|m_S\rangle$ basis. This leads to the following two Kramers doublets:

$$W_1 = \tfrac{5}{4}D + (D^2+3E^2)^{1/2} \tag{3}$$

$$|\Psi_1\pm\rangle = \sin\Theta\,|\mp\tfrac{1}{2}\rangle + \cos\Theta\,|\pm\tfrac{3}{2}\rangle\,,$$

and

$$W_2 = \tfrac{5}{4}D - (D^2+3E^2)^{1/2} \tag{4}$$

$$|\Psi_2\pm\rangle = \cos\Theta\,|\mp\tfrac{1}{2}\rangle - \sin\Theta\,|\mp\tfrac{3}{2}\rangle\,,$$

in which θ is defined by

$$\tan 2\Theta = \sqrt{3}\,E/D\,.$$

Clearly W_2 represents the Kramers ground doublet.

Subsequently, the Zeeman term in (2) is treated as a perturbation and this leads to the following effective g factors for W_2:

$$\begin{aligned} g_z^{\rm eff} &= g_z[2(1+3\alpha^2)^{-1/2} - 1] \\ g_x^{\rm eff} &= g_x[1 + (1-3\alpha)(1+3\alpha^2)^{-1/2}] \\ g_y^{\rm eff} &= g_y[1 + (1+3\alpha)(1+3\alpha^2)^{-1/2}]\,, \end{aligned} \tag{5}$$

and for W_1:

$$\begin{aligned} g_z^{\rm eff} &= g_z[1 + 2(1+3\alpha^2)^{-1/2}] \\ g_x^{\rm eff} &= g_x[1 - (1-3\alpha)(1+3\alpha^2)^{-1/2}] \\ g_y^{\rm eff} &= g_y[1 - (1+3\alpha)(1+3\alpha^2)^{-1/2}]\,, \end{aligned} \tag{6}$$

in which $\alpha = E/D$. The expressions (5) and (6) are presented graphically in Figs. 4(a) and (b), respectively. The absolute values have been presented because this is what is experimentally determined.

If we assume for simplicity that the g tensor in (2) is isotropic (a reasonable first approximation for an S state), it is seen from (5) or Fig. 4(a) that for $E=0$

$$g_\perp^{\rm eff}/g_\parallel^{\rm eff} = 2\,. \tag{7}$$

The $g^{\rm eff}$ values in the upper half of Table I for Sn^- (tetrag) obey (5) and (7) quite accurately with $g=1.981$.

Similarly, the $g^{\rm eff}$ components of Sn^- (ortho, 1) and Sn^- (ortho, 2) are reproduced quite accurately in Fig. 4(a) for $\alpha=0.14$, $g=1.954$ and $\alpha=0.19$, $g=1.950$, respectively. It should be noted that not only are the observed $g^{\rm eff}$ components of the Sn^- (tetrag) and Sn^- (ortho) EPR spectra naturally and effortlessly explained, but they each yield true g

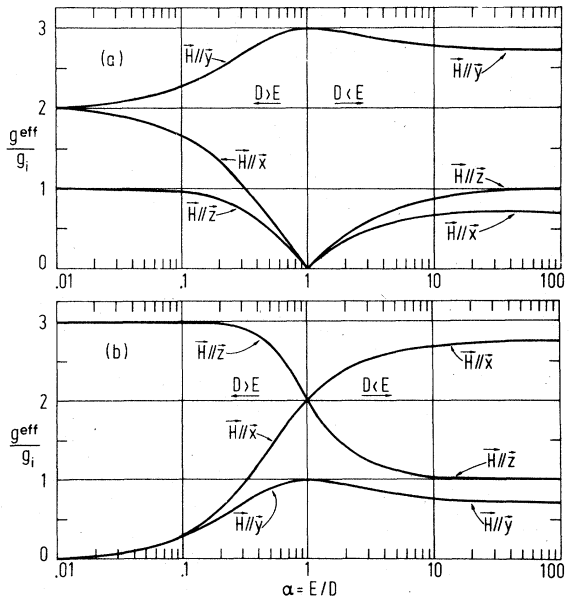

FIG. 4. $g^{\rm eff}/g_i (i=x,y,z)$ vs E/D for (a) the lowest Kramers doublet originating from a crystal-field split Γ_8, and (b) the excited Kramers doublet.

factors which are comparable to the isotropic g factor of Sn^- (cubic). The overall agreement is compelling and strongly supports our conclusion that the basic species underlying the Sn^- (cubic), Sn^- (tetrag), and Sn^- (ortho) centers is indeed a Sn^- ion possessing an $^4S_{3/2}$ ground state. In Sec. IIIB 7 the g value of a Sn^- will be discussed and its magnitude will be shown to be just what one would expect.

Finally, the experimentally observed splitting δA_α between the hf lines is related to the hf parameter $A_\alpha^{\rm eff}$ in the $S=\frac{1}{2}$ description (1) by

$$A_\alpha^{\rm eff} = (g_\alpha^{\rm eff}/g_0)\delta A_\alpha ,$$

while in the $S=\frac{3}{2}$ description (2) they are related by

$$A_\alpha = (g_\alpha/g_0)\delta A_\alpha ,$$

and thus

$$A_\alpha = (g_\alpha/g_\alpha^{\rm eff})A_\alpha^{\rm eff} .$$

Both results are quoted in Table I, but it is clear that the A_α parameters are the more fundamental ones.

4. Excited Kramers doublets: Estimate of D and E

From the Sn^- (tetrag) ESR data we can conclude that $D > (g/g_0)H$, but the value of D cannot be obtained. Similarly, for the two Sn^- (ortho) centers it can be deduced that $E/D = 0.14$ and 0.18, but the values of E and D cannot be extracted from the data.

However, if D and/or E would be of the order of a few cm^{-1} then the excited Kramers doublet W_1 would be sufficiently populated and its ESR spectra should be observable. We will discuss the case of Sn^- (ortho, 1) in some detail. Using $\langle g\rangle = 1.954$ and $\alpha = 0.14$ as determined from the lowest doublet W_2, one calculates from (6) the following $g^{\rm eff}$-values for the excited doublet W_1:

$$g_z^{\rm eff} = 5.98 , \quad g_x^{\rm eff} = 0.79 , \quad g_y^{\rm eff} = 0.90 ,$$

and hence $g^{\rm eff}(\theta = 45^\circ, \varphi = 0^\circ) = 4.27$.

Inspection of the usual experimental geometry, i.e., the microwave field $\vec{h}$ perpendicular to the external field $\vec{H}$ and a sample cut along the $\{100\}$ planes and rotating around a $\langle 100\rangle$ axis parallel to $\vec{h}$, leads to the conclusion that the $g_y^{\rm eff} = 0.90$ line should be the most intense, its intensity being proportional to $g_2^2 \equiv [g^{\rm eff}(\theta = 45^\circ, \varphi = 0^\circ)]^2 \cong 18$. For the corresponding $g_y^{\rm eff} = 4.652$ line of the ground doublet the intensity is proportional to $g_1^2 \equiv [g^{\rm eff}(\theta = 45^\circ, \varphi = 0^\circ)]^2 = (2.498)^2 \cong 6$. Designating the intensities of the corresponding lines by I_2 and I_1, the energy difference ΔW between the two Kramers doublets is given by

$$\Delta W = -k_B T \ln(g_1^2 I_2/g_2^2 I_1) .$$

Careful searches have not revealed any transitions that can be ascribed to the excited W_1 doublet, in particular the $g_y^{\rm eff} = 0.90$ transition. Taking as a lower limit for I_2/I_1 the observed signal-to-noise ratio ($\sim$100:1) at $T = 8$ K, one finds as a lower limit for ΔW (in cm^{-1})

$$\Delta W > 20 \ cm^{-1}$$

and, because $\Delta W = 2D(1+3\alpha^2)^{1/2}$ with $\alpha = 0.14$, the lower limit for D is

$$D > 17 \ cm^{-1} .$$

Although this reasoning was done specifically for Sn^- (ortho, 1) it is likely that the same lower limits apply to Sn^- (tetrag) and Sn^- (ortho, 2) because also in these cases no transitions were found that can be ascribed as originating from the excited W_1 doublet.

In a simple crystal-field approximation the value of D is given by[14]

$$D \approx \tfrac{3}{4}\lambda(g_0 - g_\parallel) \qquad (8)$$

in which $\lambda = (1500 \pm 500) \ cm^{-1}$ is the estimated value of the spin-orbit coupling constant of a $5p$ Sn^- electron. The $g_\parallel$ and $g_\perp$ values as given in the lower half of Table I are, in our opinion, not precise enough to make a meaningful individual estimate of D using (8). Taking the average of $g_\parallel$

TABLE II. ESR parameters (linewidth ΔH in units of 10^{-4} T) of Sn^- (cubic) in various alkali halides. The F-center ESR linewidths are included for comparison.

Crystal	g	$\Delta H(Sn^-)$	$\Delta H(F)$ [a]	$\Delta H(F)/\Delta H(Sn^-)$
RbCl	1.996	110	399	3.6
KCl	1.9700	18	46	2.6
NaCl	1.969	50	137	2.7
RbBr	1.976	50	360	7.2
KBr	1.967	34	124	3.6
KI	1.964	62	213	3.4

[a] From Ref. 16.

for the three anisotropic Sn^- centers yields $D \approx 27\ cm^{-1}$.

5. Sn^0 species

Having obtained a rough idea of the magnitude of the crystal field splittings for the low-symmetry Sn^- defects it is appropriate at this point to discuss the Sn^0 species. This species plays an important role in this work as will become progressively clear in Secs. IV–VIII. For at least one such defect, called Sn^0 (tetrag) (see Sec. V), there is compelling evidence that it exists and is stable at room temperature. Sn^0 is a non-Kramers $S=1$ system and a crystal field of sufficiently low symmetry will lift the degeneracy completely, or if it does not, the resulting Zeeman levels will have a zero transition probability associated with them.[15] If these crystal-field splittings are larger than the microwave energies employed, then no ESR transitions can be induced. We believe that this is the case here for Sn^0.

It is not unreasonable to assume that, roughly speaking, the crystal-field splittings in Sn^- and Sn^0 should be comparable in magnitude because we are dealing with similar electrons ($5p$) and comparable large spin-orbit interactions for both systems. In the foregoing Sec. III B 4 it was demonstrated that these crystal-field splittings are at least $\sim 20\ cm^{-1}$. If the Sn^0 splittings are comparable to this value, or even an order of magnitude smaller, then no ESR transitions can be induced at X-band frequencies ($\nu \approx 9.2$ GHz). Since we have not found any ESR signals that can be attributed to Sn^0, we believe that the foregoing discussion must be essentially correct.

6. Sn^- (cubic) in other alkali halides

Having identified the basic species underlying the four defects in KCl as being essentially Sn^-, it is reasonable to conclude that they occupy negative ion sites in the crystal instead of the positive-ion sites that the Sn^{2+} occupy before x irradiation. How this change in position may come about is discussed in Sec. VII. Here we merely want to present additional data supporting the negative-ion position of Sn^-.

To this end, the Sn^- (cubic) ESR spectrum was investigated in several Sn^{2+} doped alkali halides such as KCl, NaCl, RbCl, KBr, KI, and RbBr. The underlying idea was to compare the Sn^- (cubic) linewidth with the F-center ESR linewidth[16] because it seemed reasonable that they should roughly scale with one another. Indeed, in both cases we are dealing with S-type ground states and the linewidths are determined by hf interaction with the nuclei surrounding the negative-ion site. Because in Sn^- (cubic) the electron is expected to be more localized on the tin, the Sn^- (cubic) should possess a smaller linewidth than the F center.

The isotropic Sn^- (cubic) ESR spectra in all the alkali halides investigated were produced by x irradiation at room temperature. The experimental data are presented in Table II. First it should be noted that the isotropic g values are all very close to one another and, in particular, close to the value observed in KCl, substantiating the conclusion that all these centers are indeed Sn^- (cubic) defects. Second, it is observed that the Sn^- (cubic) linewidths scale very well with the F-center linewidths underscoring the fact that the Sn^- ions are indeed on negative-ion lattice sites.

The low intensity ^{117}Sn and ^{119}Sn hf doublets are not resolved from the dominant ^{even}Sn line except in the case of KCl where the linewidth is sufficiently narrow. Consequently, the hf splittings of Sn^- (cubic) could not be studied in these other non-isotope-enriched alkali halides. Because the Sn^- (tetrag) and two Sn^- (ortho) centers have linewidths virtually identical to the Sn^- (cubic) linewidth, it is concluded that in all four Sn^- centers the Sn^- ion is situated at a negative-ion site.

7. Discussion of g and A

The g tensors in the lower half of Table I are either isotropic [for Sn^- (cubic)] or seem to exhibit at most a small anisotropy [for Sn^- (tetrag) and Sn^- (ortho)] although the magnitude and sign of the latter may be disputed. We will ignore it from here on.

Both the near isotropic character and the magnitude of the g factor can be explained straightforwardly by the $^4S_{3/2}$ ground state of the free Sn^- ($5p^3$) ion. Indeed a pure S state will yield an isotropic Landé g factor $g=2.0023$. The difference with the experimentally determined g value is readily demonstrated by noting that the total angular momentum J is always a good quantum number for the free atom and that to first order the $^2P_{3/2}$ state originating from the same $5p^3$ configuration is mixed into the $^4S_{3/2}$ ground state[17]:

$$|J=\tfrac{3}{2}\rangle = (1-\beta^2)^{1/2}|^4S_{3/2}\rangle + \beta|^2P_{3/2}\rangle \qquad (9)$$

with $\beta = \xi_{5p}/15F_2$, in which ξ_{5p} is the spin-orbit coupling constant of an Sn^- electron, and the energy difference $E(^2P) - E(^4S) = 15F_2$ in which F_2 is the Slater-Condon parameter.

With the ground-state wave function (9) one calculates the following corrected isotropic g factor:

$$g = (1-\beta^2)g(^4S_{3/2}) + \beta^2 g(^2P_{3/2})\,. \qquad (10)$$

Since $g(^4S)=2$ and $g(^2P_{3/2})=\frac{4}{3}$, one finds for

KCl ($g = 1.9700$) that

$$\beta = \xi_{5p}/15F_2 = 0.21 \qquad (11)$$

which is a reasonable value as will be shown below. From atomic data[18] one determines $\xi_{5p}(Sn^+) = 2835\ cm^{-1}$ and $\xi_{5p}(Sn^0) \cong 2000\ cm^{-1}$. Hence, very roughly, $\xi_{5p}(Sn^-)$ is estimated to be $1500\ cm^{-1}$. From atomic data one can determine $15F_2 = E(^2P) - E(^4S)$, and one finds $17.250\ cm^{-1}$ for Sb^0, $22.600\ cm^{-1}$ for Te^+, and $35.000\ cm^{-1}$ for Xe^{4+}. Thus it is estimated that for Sn^-, $15F_2 \cong 11.000\ cm^{-1}$. Consequently, for the free Sn^- ion:

$$\beta = \xi_{5p}/15F_2 \cong 0.14\,,$$

which is comparable to the experimental value (11).

Because p electrons do not have any density in the nucleus, the observed isotropic hf interaction in the Sn^- centers must originate entirely from configuration interaction and exchange polarization. Its value should be comparable for the three Sn^- centers. Its sign cannot be determined from experiment.

The relative signs of A_z, A_x, and A_y in Sn^- (tetrag) and the two Sn^- (ortho) centers must be the same and equal to the sign of A in Sn^- (cubic) because otherwise no isotropic hf parameters $\langle A\rangle = \frac{1}{3}(A_z + A_x + A_y)$ of comparable magnitude are obtained for the four Sn^- centers. Table I summarizes these $\langle A\rangle$ values. Within 20% they are equal to one another, which is quite reasonable.

IV. MODELS FOR THE Sn^- CENTERS

In Sec. III it was established that the basic entity underlying the four observed Sn^- centers is a Sn^- ion on a negative-ion site. The experiments to be described in Secs. V and VI are meant in part to substantiate plausible models for the Sn^- defects. The volume and complexity of these data make it advisable to discuss them in terms of established or plausible Sn^- models, because otherwise the purpose of the particular experiments is easily lost.

A. Sn^- (cubic) model

For Sn^- (cubic), the model can be derived from the ESR data. The ESR spectrum, which is isotropic even at the lowest temperatures (4.2 K in one experiment), implies perfect cubic symmetry. Thus Sn^- (cubic) must be a Sn^- ion occupying a single negative-ion site not perturbed by the presence of any entity (vacancy, interstitial) in its neighborhood (Fig. 5). The Sn^- thus experiences a crystal field of perfect octahedral symmetry. The spin degeneracy of $^4S_{3/2}(\Gamma_8)$ is not lifted and as a result the ESR spectrum should not show any fine-structure splitting and should be characterized by a line whose position and hf splitting are isotropic, as is indeed observed.

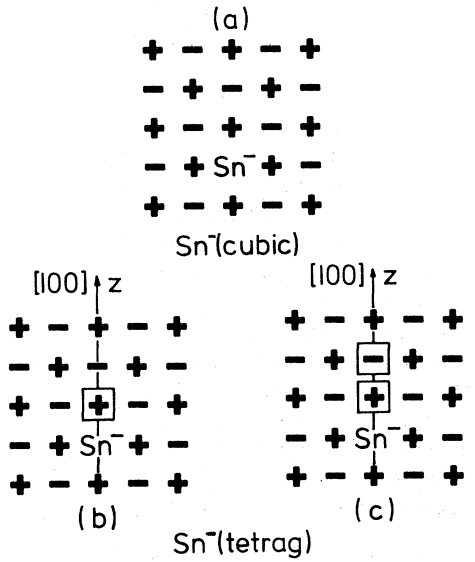

FIG. 5. Schematic models of (a) the Sn^-(cubic) center, (b) and (c) the two most plausible models for the Sn^-(tetrag) centers. It is possible that both defects (b) and (c) exist.

B. Sn^- (tetrag) model

The model for Sn^- (tetrag) cannot be unambiguously derived from the ESR data. The axial symmetry around $\langle 100\rangle$ of the ESR spectra implies tetragonal symmetry around $\langle 100\rangle$ for the Sn^- (tetrag) center. It is clear that the Sn^- must be perturbed by one or more defects or impurities along $\langle 100\rangle$. Interstitial halogens as perturbing entities should not be considered; it is hard to construct with them Sn^- centers of perfect tetrahedral symmetry around a $\langle 100\rangle$. Although the possibility cannot be excluded that the perturbing defect is a substitutional impurity ion, the arguments to be presented later in this paper strongly favor the conclusion that the perturbing entity is composed out of one or more vacancies.

The two most plausible models for Sn^- (tetrag) are presented schematically in Figs. 5(b) and (c): either a single positive-ion vacancy along $\langle 100\rangle$ perturbs the Sn^- or a divacancy pair along $\langle 100\rangle$ does. Note that once $D > h\nu$, two Sn^- (tetrag) defects with quite different values of D might not be distinguishable in ESR because the g^{eff} values are insensitive to the magnitude of D. Only if the real g values would be sufficiently different could the difference in ESR spectra be noticeable.

The experiments to be described in Secs. V and VI really do not permit us to make a definite

choice between the two models of Figs. 5(b) and (c). If the strong decay of Sn^- (tetrag) under optically or thermally induced decay of the V_K center would mean that Sn^- (tetrag) is negatively charged then the model of Fig. 5(b) would be strongly favored. If the strong production of Sn^- (tetrag) under optical F-center excitation at 10 K would mean that the Sn^0 (tetrag) precursor (see Sec. V) should be positively charged, then the model of Fig. 5(c) would be favored. However many neutral centers, such as, Tl^+, Br^-, and Pb^{2+} (the latter compensated by a positive-ion vacancy) are known to possess large cross sections for trapping holes and electrons. Thus the behavior under hole or electron trapping does not necessarily yield the effective charge of a defect. In fact neither model of Fig. 5 is in contradiction to either the F- or V_K-center bleach data.

C. Sp^- (ortho, 1) and Sn^- (ortho, 2) models

Finding definite models for these two Sn^- (ortho) centers or even narrowing the possibilities down to a few plausible models is difficult. If the z axes of Sn^- (ortho, 1) and Sn^- (ortho, 2) would be oriented perfectly along ⟨110⟩ then the three models presented in Figs. 6(a)–(c) would represent possible and plausible models. In these models the vacancies induce a dominant tetragonal crystal-field component DS_z^2 along ⟨110⟩ and the ionic displacements are responsible for the orthorombic component $E(S_x^2 - S_y^2)$.[19] We believe that one or more of these models must represent the essential core of the Sn^-(ortho) centers. However, because for both centers the z axes make small angles with ⟨110⟩ in a {100} plane there must be one or two other perturbing defects (very likely vacancies) in the neighborhood of this essential core immediately outside the area designated by the circle. The possibilities are *a priori* numerous and the experiments described in Secs. V–VII have not permitted us to be more specific, except for the general observation that the two Sn^- (ortho) centers are quite different from one another in the sense that a simple single or double jump of a vacancy around the Sn^- is not sufficient to go from Sn^- (ortho, 1) to Sn^- (ortho, 2) or vice versa. This conclusion is based on the observation that these two defects are never seen to go over into one another.

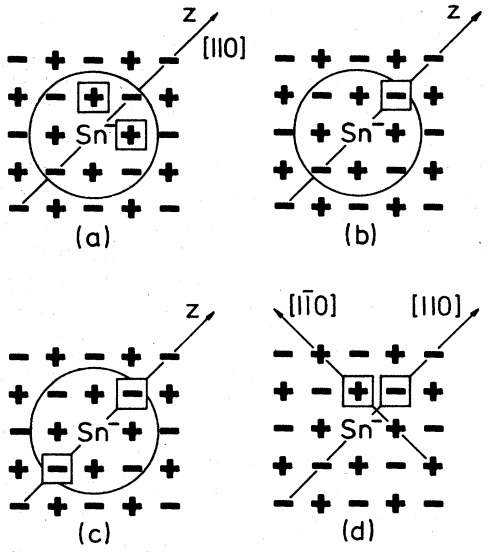

FIG. 6. (a), (b), and (c) three possibilities of the essential core (within the circle) of Sn^-(ortho) defects. For both Sn^-(ortho, 1) and Sn^-(ortho, 2) there must be at least one other perturbing entity, most likely another vacancy, outside this core; (d) simple and compact Sn^- defect model which ought to exist but for which it is argued that it cannot represent a possible model for either Sn^-(ortho, 1) or Sn^-(ortho, 2).

One possible Sn^- center model, namely, the one presented in Fig. 6(d) involving two vacancies merits a discussion. Because it is a simple and compact model, one feels that it ought to exist. One can look upon this model as being the Sn^- (tetrag) center of Fig. 5(b) perturbed by the presence of a negative-ion vacancy along ⟨110⟩. Thus one expects such a configuration to result in a small tipping of the z axis away from ⟨100⟩ rather than a small tipping away from ⟨110⟩ as is observed for the two Sn^- (ortho) centers. For this reason the model of Fig. 6(d) is not seriously considered as a model for one of the Sn^- (ortho) defects. However, one might argue that it would still be possible to obtain a small tipping away from ⟨110⟩ in this case by assuming that the Sn^- moves along [110] away from the negative-ion site, but not quite reaching the intersection of the [110] and [1$\bar{1}$0] directions. For such a model one would expect a jumping motion of the Sn^- between the two equivalent positions with respect to the [1$\bar{1}$0] direction which, when fast enough at sufficiently high temperatures, would essentially average out the tipping. However, no motional averaging effects were observed in the Sn^- (ortho) ESR spectra. Thus we conclude that the model of Fig. 6(d) is not a plausible model for either one of the Sn^- (ortho) centers.

Still, because of its simplicity and compactness it seems likely that the model of Fig. 6(d) exists as a Sn^- defect. Possible motional effects may have broadened the lines even at 8 K where most ESR measurements were done, making it in fact an unobservable Sn^- defect (see Sec. VII).

Finally, it is useful for the discussion in the next section to recall briefly in Figs. 7(a)–(c) the established models for the Sn^+ centers,[6] namely,

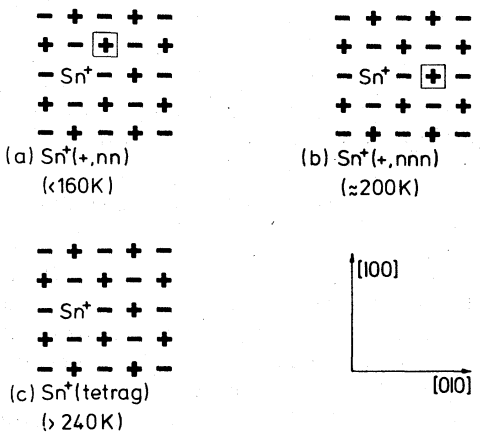

FIG. 7. Schematic model for the three Sn^+ centers (from Ref. 6). These Sn^+ centers manifest themselves as linear symmetric $SnCl_2^-$ molecules; the molecular axis is oriented perpendicular to the plane of the figure.

$Sn^+(+,nn)$, $Sn^+(+,nnn)$, and Sn^+ (tetrag) which are produced by x irradiation at 77 K and a simple warm-up. (nn and nnn stand for nearest neighbor and next nearest neighbor, respectively).

V. SOME PRODUCTION, THERMAL, AND PHOTOCHEMICAL PROPERTIES

A. Production curves

1. X irradiation at 77 K

No Sn^- defects are observed in ESR after x irradiation at 77 K or after a subsequent warm-up to room temperature. Because it is reasonable to assume that an Sn^- production sequence must involve a Sn^0 species, this experiment could suggest that the $Sn^+(+,nn)$ defect which is predominantly produced by x irradiation at 77 K, does not trap another electron and thus is not the start of a production sequence resulting in Sn^- defects.

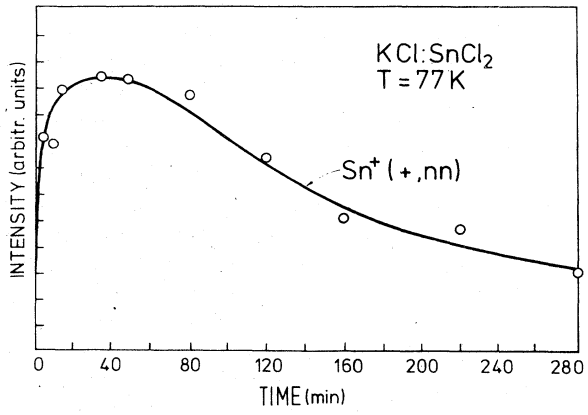

FIG. 8. Production at 77 K of the $Sn^+(+,nn)$ defect of Fig. 7 (a) as a fuction of x irradiation time.

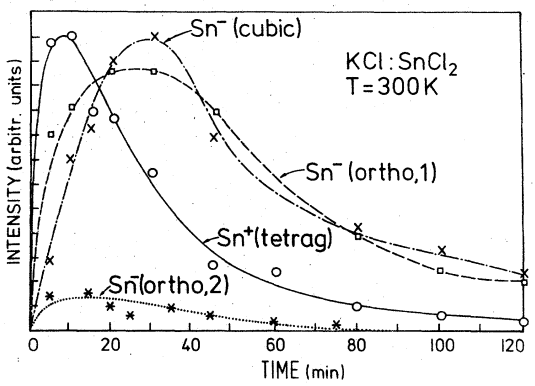

FIG. 9. Production at room temperature of the Sn^+(tetrag), Sn^-(cubic, Sn^-(ortho, 1), and Sn^-(ortho, 2) defects as a function of x irradiation time.

However, it is also quite possible that there are so many other competing electron traps at 77 K that the probability that $Sn^+(+,nn)$ traps another electron is small. Figure 8 presents the production of $Sn^+(+,nn)$ at 77 K by the x irradiation. The $Sn^+(+,nn)$ concentration reaches a maximum after about 40 min after which it decays slowly.

2. X irradiation at room temperature

This irradiation produces Sn^+ (tetrag), Sn^- (cubic), Sn^- (ortho, 1), and a small amount of Sn^- (ortho, 2). The production of these defects is given in Fig. 9. Noteworthy are (i) the rapid production of Sn^+ (tetrag) reaching a maximum after about 10 min after which it decays fast and (ii) the distinctly slower production of Sn^- (cubic) and Sn^- (ortho, 1) which both reach a maximum after about 30 min at which time Sn^+ (tetrag) is already strongly decaying. The production before this maximum and the decay afterwards proceed with comparable rates for both Sn^- defects.

This production curve is consistent with the assumption that at least one of the production mechanisms of the Sn^- defects proceeds via the Sn^+ (tetrag) centers. In contrast to 77 K, positive- and negative-ion vacancies are mobile at room temperature; also the F centers are no longer competing electron traps because F' centers are thermally unstable above 200 K.[20,21]

3. X irradiation at room temperature followed by irradiation at 77 K

If a sample is irradiated for about 5 min at room temperature and then studied at 77 K as a function of x irradiation time, one obtains the data of Fig. 10. Noteworthy are the very rapid production of Sn^- (tetrag) reaching a maximum after about 5 to 10 min and the rapid decay afterwards. This very fast production strongly in-

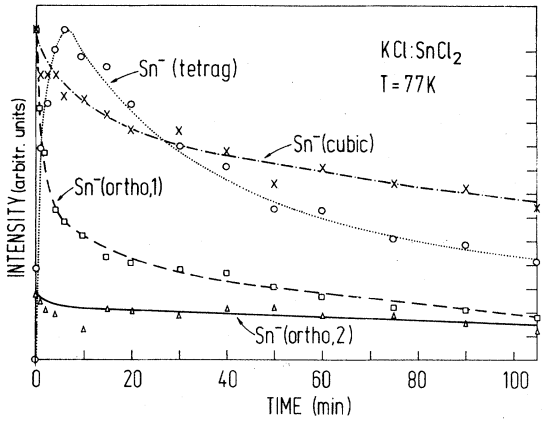

FIG. 10. Formation and/or behavior of Sn^-(cubic), Sn^-(tetrag), Sn^-(ortho, 1), and Sn^-(ortho, 2) under x irradiation at 77K after the crystal had been irradiated for 5 min at room temperature.

dicates that Sn^- (tetrag) is produced by an electronic process, i.e., by simple trapping of an electron or a hole rather than the trapping of interstitials, the production of which proceeds at a much slower rate. Saturation concentrations of halogen interstitial centers are reached only after a few hours of x irradiation.

Looking at the model for Sn^- (tetrag) in Fig. 5(b), this experiment implies that the x irradiation at room temperature has produced precursor centers which after trapping of an electron become Sn^- (tetrag). This precursor center, designated Sn^0 (tetrag), is presented schematically in Fig. 11(a). Whether before electron trapping the Sn^0 is on the negative- or on the positive-ion site is a moot question at this point. Precursors which yield Sn^- (tetrag) after hole trapping are less likely. In fact the decay of Sn^- (tetrag) after about 10 min may well be caused predominantly by hole trapping (see Secs. V B and VI) reproducing the Sn^0 (tetrag) precursor. Figure 10 also shows that Sn^- (cubic), which is strongly produced by the x irradiation at room temperature, decays under irradiation at 77 K, presumably by hole trapping, although trapping of interstitial halogens cannot

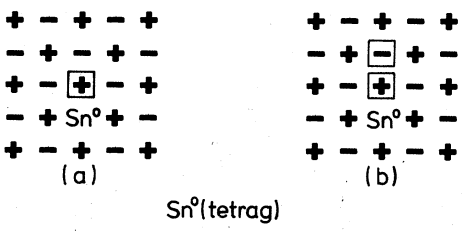

FIG. 11. Schematic models for the Sn^0(tetrag) defects which are the precursors under electron trapping of the two Sn^-(tetrag) models of Fig. 5.

be excluded.

Sn^- (ortho, 1) decays very fast initially, pointing to annihilation by electron or hole trapping. Sn^- (ortho, 2), on the other hand, is not much affected, possibly because of its low concentration.

B. Behavior under optical V_K-center excitation

Because the Cl_2^- V_K centers (or "self trapped hole" centers) are not stable at room temperature (the decay temperature is[22] −60 °C) a V_K center containing sample was produced as in Sec. V A 3, namely, 10 min x irradiation at room temperature [which produces Sn^- (cubic), Sn^- (ortho, 1), Sn^- (ortho, 2) and, we believe, the Sn^0 (tetrag) precursor] followed by a 10-min x irradiation at 77 K. The latter produces Cl_2^- V_K centers, F' centers, and Sn^- (tetrag) centers (see Fig. 10). The results of an optical V_K-center excitation at 10 K using 335-nm light are readily summarized: a sharp parallel drop of both V_K and Sn^- (tetrag) within the first minute of excitation, while Sn^- (ortho, 1), Sn^- (ortho, 2), and Sn^- (cubic) show only a small decrease.

This strong decay of Sn^- (tetrag) when positive holes are freed would favor the negatively charged model of Fig. 5(b) for the Sn^- (tetrag) defect if it could be assumed that the Sn^- (tetrag) defect occurs with a low concentration compared to other competing electron traps. This, however, is not readily ascertained. The neutral Sn^- (tetrag) model of Fig. 5(c) can, if present in sufficient abundance, equally well trap positive holes.

The fact that no Sn^- centers are produced by a V_K-center bleach leads to the conclusion that there exist no precursor centers which after hole trapping result in the formation of Sn^- defects. From here on the term precursor will mean precursor center under electron trapping.

C. Behavior under optical F-center excitation

An F-center bleach (which produces mobile electrons) at 10 K of a sample irradiated only at room temperature (i.e., same treatment as for Fig. 9) yields the following results: practically no change for Sn^- (cubic), Sn^- (ortho, 1), and Sn^- (ortho, 2) but, within a period of 30 sec to 1 min, a strong production of Sn^- (tetrag). One concludes that only a precursor for Sn^- (tetrag), called Sn^0 (tetrag), is produced in substantial quantities by the x irradiation at room temperature, while no precursors for Sn^- (cubic), Sn^- (ortho, 1), and Sn^- (ortho, 2) are formed. This latter conclusion is rather compelling for Sn^- (cubic), because its precursor, namely, a Sn^0 on a negative-ion site would be expected to exert a strong attractive force on the mobile electrons. This absence of precursors

except for Sn^- (tetrag) is confirmed by other experiments later on and is important. It points to a central role played by Sn^- (tetrag) and its Sn^0 (tetrag) precursor in the production of Sn^- defects. After a bleach of about 1 min a saturation in the Sn^- (tetrag) concentration is reached. The reason is that the Sn^0 (tetrag) precursors have all been used up and not because there are no F centers anymore. This is illustrated by a subsequent experiment on the same sample. A warm-up to room temperature destroys the Sn^- (tetrag) centers ($T_{decay} = -20$ °C, see Sec. VI). The decay occurs because they are transformed into the other Sn^- centers (most likely by the trapping or loss of one or more vacancies), not because they lose an electron. Yet this warm-up clearly produces, by another mechanism, new Sn^0 (tetrag) precursors, because Sn^- (tetrag) centers are again strongly produced by a subsequent F-center excitation at 10 K. This process can be repeated several times (see Fig. 12) until finally after five or more such cycles no more Sn^- (tetrag) centers are produced, because there are no more F centers left (see Sec. VI B 2).

The rapid production of Sn^- (tetrag) under F excitation indicates that its precursor is either positively charged, leading to a neutral Sn^- (tetrag) [Fig. 5(c)], or neutral, leading to a negatively charged Sn^- (tetrag) [Fig. 5(b)]. Again these measurements do not permit us to make a definite choice between the two.

It is possible that both Sn^- (tetrag) possibilities of Figs. 5(b) and 5(c) occur simultaneously, but that they cannot be distinguished experimentally in ESR because once $D > h\nu$ the ESR spectra are quite insensitive to the value of D.

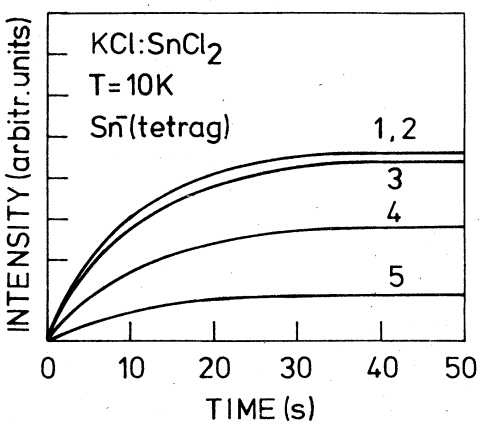

FIG. 12. Effect of an optical F-center bleach at 10 K using 530-nm light. Prior to this the crystal had been x irradiated for about 10 min at room temperature in order to produce Sn^0 (tetrag) precursors. After the F bleach, the sample was brought to room temperature and this cycle was repeated four times.

VI. PULSE-ANNEAL RESULTS

A. X irradiation at 77 K after X irradiation at 300 K

Figure 13 presents pulse-anneal data between 160 and 440 K on a KCl:Sn^{2+} sample which had been x irradiated at room temperature followed by an x irradiation at 77 K. Such a treatment produces, besides the four Sn^- defects, V_K, F, and F' centers. Nothing happens between 77 and 170 K. Then around 210 K, the Cl_2^- centers decay and parallel with it the Sn^- (tetrag) concentration drops substantially. This Sn^- (tetrag) decay is interpreted in the same way as under optical V_K center excitation: the mobile positive holes are trapped by the Sn^- (tetrag) centers producing the Sn^0 (tetrag) precursor.

In this experiment there is also a drop in Sn^- (cubic) when Cl_2^- decays. This is not inconsistent with the neutral character of Sn^- (cubic). Both Sn^- (ortho, 1) and Sn^- (ortho, 2) remain untouched under V_K-center decay possibly because of their lower concentration although just above this region Sn^- (ortho, 1) starts to increase. The reason for this may be the following. F' centers become thermally unstable in this region (>200 K) releasing electrons. Some Sn^- (ortho, 1) have trapped holes produced by the 77-K irradiation thus producing some amount of Sn^0 (ortho, 1) precursors. These can trap the liberated F'-center electrons and reform Sn^- (ortho, 1).

The increase of Sn^- (ortho, 1) continues in the temperature region 240 to 260 K together with

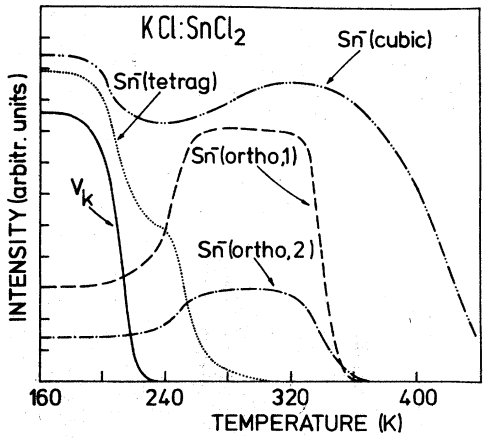

FIG. 13. Pulse-anneal results on a KCl:Sn^{2+} sample which had been x irradiated at room temperature for 5 min followed by a 10-min x irradiation at 77 K (see Fig. 10). At every temperature the crystal was held for 5 min and then cooled to 10 K, where the changes in the ESR spectrum were measured. The relative intensities of the centers are arbitrary, except maybe for the two Sn^-(ortho) centers.

Sn^- (ortho, 2) and Sn^- (cubic), while Sn^- (tetrag) virtually decays completely. We believe that the latter center is converted directly or indirectly into the former three centers and that Sn^- (tetrag) and its precursor play an important role in a production sequence of the Sn^- defects. Finally, Sn^- (ortho, 1), Sn^- (ortho, 2) both decay at 335 K and Sn^- (cubic) at 400 K. Noteworthy is the fact that neither Sn^- (ortho, 1) nor Sn^- (ortho, 2) are converted into one another or into Sn^- (cubic) when they decay. The decay mechanisms of these centers are not known and were not further investigated.

B. X irradiation at 200 K

1. Simple pulse anneal

Figure 14 presents data of another remarkable pulse-anneal experiment performed on a sample which had been irradiated at 200 K. The reason for this particular experiment was the following. Neither an x irradiation at 77 K nor a subsequent warm-up to room temperature produces Sn^- centers. Because only Sn^+ (+, nn) [see Fig. 7(a)] is produced at 77 K, it was concluded that it does not initiate a production sequence leading toward Sn^- defects. However, at 200 K most Sn^+ (+, nn) has been converted to Sn^+ (+, nnn)[6] [Fig. 7(b)]. To see whether the latter might lie at the basis of some Sn^- defects, a sample was x irradiated at 200 K and a subsequent pulse anneal was performed. It should also be remarked that F' centers are thermally unstable at 200 K so that F centers are eliminated as competing electron traps. Also at 200 K one approaches the temperature region where negative-ion vacancies become mobile[20,23,24] (>220 K).

The x irradiation at 200 K does not produce observable Sn^- defects just as in the case of irradiation at 77 K. Yet there is a difference, because the 200-K irradiated sample *does* produce Sn^- defects after a warm-up to room temperature. In another respect the two samples behave similarly: optical F-center excitation at 10 K does not produce Sn^- (tetrag) indicating that, although something quite different happened by x irradiation at 200 K, the Sn^0 (tetrag) precursor was not yet formed.

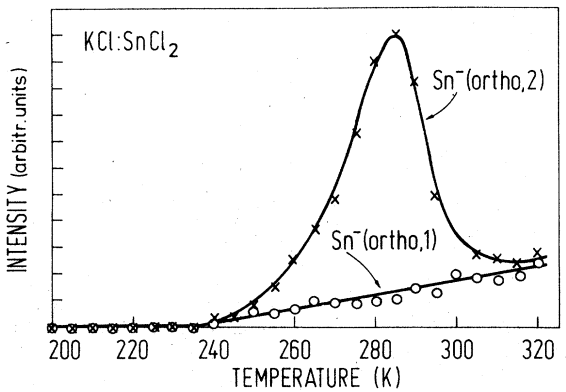

FIG. 14 Pulse-anneal results on a KCl:Sn^{2+} sample which had been x irradiated for 10 min at 200 K.

In order to study these phenomena further a pulse anneal was performed on the 200-K x-irradiated sample. The data are presented in Fig. 14. Between 200 and 230 K nothing appears to happen. This, however, is not true. A sample brought to 230 K after x irradiation at 200 K, and subsequently optically excited in the F band at 10 K, produces Sn^- (tetrag) in quite observable quantities. Thus the Sn^0 (tetrag) precursor has been formed by the warm-up to 230 K pointing to sufficiently fast negative-ion vacancy motion around 230 K.

Above 240 K the two Sn^- (ortho) centers form although at different rates and with different intensities. Because the two Sn^- (ortho) centers are so similar in nature the relative intensities in the figures are likely to be roughly correct. Sn^- (ortho, 2) rises rapidly, reaching a maximum near 280 K after which a large fraction decays around 290 K. Sn^- (ortho, 1) on the other hand, rises slowly and monotonically in the same temperature region and is much less intense. The great difference in production rate and the fact that the substantial decay of Sn^- (ortho, 2) at 290 K does not result in production of Sn^- (ortho, 1) leads one to conclude that both Sn^- (ortho) centers must differ in an essential way from one another. If it were simply a matter of a rearrangement of vacancies around the Sn^- then one or two elementary jumps of vacancies might convert one into the other. This experiment suggests that the number, type, and arrangement of the vacancies are essentially different for the two Sn^- (ortho) defects.

The fact that both Sn^- (ortho) centers start to form at 240 K, which happens to be the region where the positive-ion vacancy starts to become mobile,[25,26] may or may not be coincidental. This point will be discussed in Sec. VII.

The very sharp drop of Sn^- (ortho, 2) around 290 K indicates that Sn^- (ortho, 2) decays already in the range 275–280 K but that in that region its decay is still overwhelmed and compensated by the hitherto unknown mechanism that produces Sn^- (ortho, 2).

2. Isothermal anneal at 273 K

The data presented in Fig. 15 were obtained from an experiment motivated by the results of the

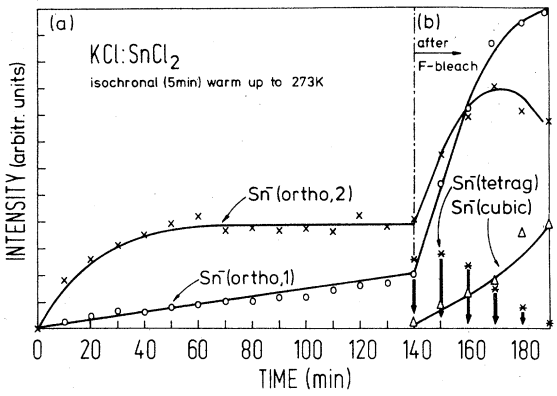

FIG. 15. (a) Production as a function of time of Sn^-(ortho, 1) and Sn^-(ortho, 2) at 273 K in a sample which had been x irradiated at 200 K for about 10 min. (b) Continuation of the same pulse anneal at 273 K but now preceded each time by an optical F-center excitation at 10 K (see Fig. 12) which produces Sn^-(tetrag); the latter drops to zero each time at 273 K, and Sn^-(cubic), Sn^-(ortho, 1), and Sn^-(ortho, 2) are produced.

foregoing experiment. Here a KCl:Sn^{2+} sample was irradiated at 200 K followed by an isochronal (5 min for every point) and isothermal anneal at 273 K and measured in ESR at 10 K. It is seen that, in agreement with Fig. 14, Sn^- (ortho, 2) is formed strongly but that its intensity reaches a saturation value after about 60 min. Sn^- (ortho, 1), on the other hand, grows slowly and keeps on growing even after two hours. Since the experiment of Fig. 14 showed that the precursor Sn^0 (tetrag) was formed at and above 230 K, the following was done after 140 min of anneal at 273 K. A saturation concentration of Sn^- (tetrag) was produced at 10 K by optical excitation in the F band and the Sn^- (tetrag) intensity thus obtained is indicated rather arbitrarily by the crosses in the right-hand side of Fig. 15. A warm-up to 273 K destroys the Sn^- (tetrag) ($T_{decay} = 255$ K), but Sn^- (ortho, 1) and Sn^- (ortho, 2) increase strongly in intensity and Sn^- (cubic) is formed. This cycle can be repeated several times [see Fig. 15(b)] until, after the sixth F bleach in this experiment, virtually no more Sn^- (tetrag) is produced. The reason is that most of the F centers have been used up. This is clear to the eye because after the fifth treatment the sample is transparent and does not exhibit anymore the characteristic blue F-center color.

In trying to interpret the data of Fig. 15 one should keep in mind the likelihood that F-center excitation at 10 K may produce F' centers. These decay around 200 K and could also play a role in the production of the Sn^- (ortho) and Sn^- (cubic) centers. Furthermore, the bleaching of F centers has produced negative-ion vacancies which become mobile above 220 K and these too might contribute to the production of Sn^- (ortho, 1) and Sn^- (ortho, 2). Still the data of Fig. 15 are suggestive in indicating that there is a production sequence leading to the Sn^- (ortho, 1), Sn^- (ortho, 2), and Sn^- (cubic) centers which passes via the Sn^- (tetrag) centers. On the other hand, Figs. 14 and 15 indicate that, at least for Sn^- (ortho, 1) and Sn^- (ortho, 2) there may exist a second production sequence not involving Sn^- (tetrag), but maybe Sn^0 (tetrag) which cannot be observed; see Sec. VII.

VII. PRODUCTION MECHANISM OF Sn^- DEFECTS

The production mechanisms of the Sn^- defects are clearly very complex. In fact, the data presented in this paper and based only on ESR observations do not permit us to propose a production mechanism that we feel is exact in all its details. Also, because we do not know precisely what the models for the Sn^- (ortho) centers are [even for Sn^- (tetrag) there is some doubt], we can only propose general reaction mechanisms leading toward the Sn^- (ortho) defects.

Yet we can draw a rough outline, which is at the same time too simple and too vague in its details, but which should contain the essence of the actual mechanism. The formation of Sn^- out of Sn^{2+} must pass through Sn^+ and Sn^0 species and must involve the change of Sn^0 from a positive-ion site to a negative-ion site. This last point suggests that Sn^- defects can only be formed at and above temperatures where negative-ion vacancies are mobile, i.e., above 220 K.[20,23,24]

A reasonable production scenario at room temperature may be the following. Electrons produced by the x irradiation are trapped as F centers and by Sn^{2+} impurities forming Sn^+ (+, nn) [Fig. 7(a)]. Such a species is very unstable at room temperature. It loses its positive-ion vacancy, indicated by (+), immediately (they become mobile above 240 K)[25,26] and the defect becomes Sn^+ (tetrag):

$$Sn^+ (+, nn) - (+) \rightarrow Sn^+ (\text{tetrag}) .$$

Negative-ion vacancies, indicated by (−), also produced by the irradiation, are very mobile (indicated by { }) at room temperature and the Sn^+ (tetrag) may in rapid sequence trap one of them and another electron (or vice versa) forming a Sn^0 species on a divacancy, i.e., the Sn^0 (tetrag) species of Fig. 11(a):

$$Sn^+ (\text{tetrag}) + \{(-)\} + \{e\} \rightarrow Sn^0 (\text{tetrag}) .$$

The data presented in Secs. V and VI do indeed point strongly to a rapid and substantial production of stable Sn^0 (tetrag) precursors at room tem-

perature. This particular Sn^0 (tetrag) is compact and neutral. It is not expected to dissociate into a Sn^0 on a negative-ion site and a mobile positive-ion vacancy. The data support this because such a Sn^0 species, being the precursor for Sn^- (cubic), is apparently *not* produced either at room temperature or at the other temperatures investigated.

The Sn^0 (tetrag) precursor in Fig. 11(a) is neutral but it might still trap one or more mobile vacancies (positive and negative). However, if it does so, it will not be under the form of precursors of either one of the Sn^- (ortho) centers, because no experimental evidence for such precursors has been found, on the contrary.

Thus it appears that the next important step must be the trapping of another electron by the Sn^0 (tetrag) precursor. Because no precursors apparently exist for the Sn^- (cubic) and Sn^- (ortho) centers it appears that this electron trapping should initiate mechanisms for the production of Sn^- defects.

If the Sn^0 (tetrag) precursor traps an electron at room temperature an unstable Sn^- (tetrag) is produced (see Fig. 13) because its decay temperature is −20 °C. It may be that the released trapping energy aided by the room-temperature thermal energy is sufficient to dissociate away with some probability a mobile positive-ion vacancy, thus forming a stable Sn^- (cubic). If this is indeed a process for production of Sn^- (cubic), then the room-temperature thermal energy is necessary because production by x rays of Sn^- (tetrag) at 230 K does *not* result in the production of Sn^- (cubic) (see Fig. 3), although it is believed that at these lower temperatures the production of Sn^- (tetrag) is also caused by trapping of an electron by Sn^0 (tetrag). Of course it is quite possible that the production of Sn^- (cubic) is more complex.

If the Sn^- (ortho) defects also originate from the unstable Sn^- (tetrag), other processes must occur with a reasonable probability. In fact, rather than losing a positive-ion vacancy, the Sn^- (tetrag) could trap one or more vacancies of a suitable kind in a suitable configuration to give the observed Sn^- (ortho) defects. Because we really do not know the detailed Sn^- (ortho) structures, it is not worthwhile to elaborate on this further.

Trying to relate some of the foregoing ideas to the processes occuring in Fig. 14 is not so easy. No Sn^0 (tetrag) precursors are formed by x irradiation at 200 K, but a subsequent warm-up to 230 K does. This is quite reasonable if it is assumed that a Sn^0 (+, nnn) species is formed by the x irradiation at 200 K, i.e., a Sn^+ (+, nnn) center [Fig. 7(b)] that has trapped another electron. The Sn^0 on a positive-ion site (indicated by $Sn^0_{(+)}$), and the positive-ion vacancy in the nnn position are now repulsive and it is quite likely that the positive-ion vacancy moves away. Because negative-ion vacancies become mobile at 220 K,[20,23,24] a warm-up to 230 K may result in trapping of a negative-ion vacancy by $Sn^0_{(+)}$ thus forming the Sn^0 (tetrag) precursor in agreement with the experimental observations.

The next step in the process is less certain. One possibility is that above 240 K electrons are released which are trapped by Sn^0 (tetrag) forming Sn^- (tetrag), which in turn are then quickly converted by vacancy trapping into the Sn^- (ortho) centers. This latter conversion should occur at a very fast rate because otherwise the fact that no Sn^- (tetrag) centers are observed cannot be explained. Another drawback to this mechanism is that one needs mobile electrons above 240 K. The only known defect releasing an electron near this temperature is the F' center. However, the decay temperature of F' is usually found around 200 K which is substantially different from 240 K. If the proposed mechanism holds, one must assume either that the thermal stability of F' centers is higher in $KCl:Sn^{2+}$ than in pure KCl or that there is another, as yet unknown, electron trap releasing electrons above 240 K.

The following alternative explanation based solely on vacancy motion also has its difficulties. Positive-ion vacancies do become mobile at and above 240 K.[25,26] It is perhaps no accident that the Sn^- (ortho) defects are produced above 240 K and thus it is tempting to associate the production of the Sn^- (ortho) centers with a mechanism whereby other Sn^- defects attract at least one positive-ion vacancy and form two types of Sn^- (ortho) centers. These other Sn^- defects then must have been formed either by the irradiation at 200 K and/or by the subsequent warm-up to 240 K. However, these Sn^- are not observed in ESR above 8 K. Although this is a serious strike against it, this mechanism merits further consideration because the ESR intensities of the Sn^- (tetrag) and Sn^- (ortho) centers are themselves very strongly temperature sensitive. Above 13 K they are no longer observable. For other Sn^- defects this observational limit in temperature could very well be lower, e.g., because of rapid motional broadening of the lines. Indeed, neither Sn^- (tetrag) because of its particular structure, nor very likely the Sn^- (ortho) defects because of their low symmetry (tilting of z axes), possess degrees of freedom for motion. Other Sn^- defects with higher symmetry may have these and may thus be unobservable if the motion is sufficiently fast. This point needs further detailed study.

The partial decay of Sn^- (ortho, 2) at 295 K is

likewise difficult to explain. One thing is clear. This partial decay does not result in the formation of any of the other observed Sn^- defects, Sn^- (ortho, 1) in particular.

VIII. CONCLUSION

We have shown by studying their ESR spectra that several Sn^- defects are produced in $KCl:Sn^{2+}$ crystals by at least one short x irradiation above 200 K followed by suitable thermal and optical treatments. Detailed ESR parameters and other data were presented for four defects: Sn^- (cubic), Sn^- (tetrag), Sn^- (ortho, 1), and Sn^- (ortho, 2). For Sn^- (cubic) and Sn^- (tetrag) it proved possible to present definite or very plausible models, but for the Sn^- (ortho) defects only general suggestions regarding their essential structure could be given.

The production of Sn^-, starting from the original Sn^{2+} impurity in KCl, passes through Sn^+ and Sn^0 species. There is very compelling evidence for the existence of one particular Sn^0 defect, namely, Sn^0 (tetrag), the precursor defect of the Sn^- (tetrag) center under electron trapping. The data suggest that it plays an important role in at least one possible production sequence of the Sn^- defects. Another essential fact in the production is the mobility of the negative-ion vacancy above 220 K, otherwise the change of the tin from a positive-ion site to a negative-ion site would be very hard to explain.

It is very obvious from this work that ESR is an essential and indispensable tool in the identification and study of these and similar complex defects. Conclusions based on, e.g., optical data alone are oftentimes more speculative.[26-28]

Yet in spite of the detailed and abundant information that an ESR study yields, it is clear that one will have to draw on other experimental techniques in order to get a more complete understanding of the structure and the production of the Sn^- centers. By their very nature the production of these complex Sn^- defects must show strong similarities with the production of the complex electron centers (F and F-aggregate centers, Z centers[29]). Further progress can undoubtedly be made by combining the ESR work with optical measurements.

ACKNOWLEDGMENTS

The authors are indebted to P. H. Yuster and C. J. Delbecq from Argonne National Laboratory, A. Lagendijk for many discussions, and A. Bouwen for extensive experimental support. Support from the Belgian science funding agencies Interuniversitair Instituut voor Kernwetenschappen (IIKW), the Nationaal Fonds voor Wetenschappelijk Onderzoek (NFWO) and a NATO research grant are gratefully acknowledged. One of us (F. Van Steen) wishes to thank the Instituut tot aanmoediging van het Wetenschappelijk Onderzoek in Nijverheid en Landbouw (IWONL) for a scholarship.

[1]See, e.g., Le Di Sang, R. Romestain, Y. Merle d'Aubigné, and A. Fukuda, Phys. Rev. Lett. 38, 1539 (1977); 39, 676 (1977).
[2]C. J. Delbecq, A. K. Gosh, and P. H. Yuster, Phys. Rev. 151, 599 (1966).
[3]W. Dreybrodt and D. Silber, Phys. Status Solidi 20, 337 (1967).
[4]D. Schoemaker and J. L. Kolopus, Solid State Commun. 8, 435 (1970).
[5]N. I. Melnikov, R. A. Zhitnikov, and V. A. Khramtsov, Sov. Phys. Solid State 17, 2129 (1976).
[6]C. J. Delbecq, R. Hartford, D. Schoemaker, and P. H. Yuster, Phys. Rev. B 13, 3631 (1976).
[7]J. P. Stott and J. H. Crawford, Phys. Rev. B 4, 639 (1971).
[8](a) D. Schoemaker, E. Goovaerts, and S. Nistor, Bull. Am. Phys. Soc. 23, 200 (1978); (b) E. Goovaerts, A. Lagendijk, and D. Schoemaker, International Conference on Defects in Insulating Crystals, Gatlinburg, 1977 (unpublished).
[9]D. Schoemaker and F. Van Steen, Bull. Am. Phys. Soc. 23, 200 (1978); F. Van Steen, A. Lagendijk, and D. Schoemaker, in Ref. 8 (b).
[10]F. Fisher, Z. Phys. 231, 393 (1970).
[11]K. Kojima, M. Maki, and T. Kojima, J. Phys. Soc. Jpn. 28, 1227 (1970).
[12]A. Vanwelsenaers and D. Schoemaker, Rev. Sci. Instrum. 48, 483 (1977).
[13]W. Känzig and M. H. Cohen, Phys. Rev. Lett. 3, 509 (1959).
[14]A. Abragam and B. Bleaney, *Electron Paramagnetic Resonance of Transition Ions* (Oxford University, New York, 1970), pp. 152 and 749.
[15]Reference 14, pp. 23 and 154.
[16]J. J. Markham, *Solid State Physics*, edited by F. Seitz and D. Turnbull (Academic, New York, 1966), Suppl. 8.
[17]J. S. Griffith, *The Theory of Transition Metal Ions* (Cambridge University, Cambridge, England, 1964), p. 113.
[18]Landolt-Bornstein, *Teil Atomen und Ionen* (Springer-Verlag, Berlin, 1950), Vol. 1.
[19]G. D. Watkins, Phys. Rev. 113, 79 (1959).
[20]F. Lüty in *Physics of Color Centers*, edited by W. B. Fowler (Academic, New York, 1968).
[21]E. Sonder, W. A. Sibley, and W. C. Mallard, Phys. Rev. 159, 755 (1967).
[22]D. Schoemaker, Phys. Rev. B 7, 786 (1973).
[23]T. Matsuyama and M. Hirai, J. Phys. Soc. Jpn. 27, 1526 (1969).
[24]G. Guiliani and E. Reguzzoni, Phys. Status Solidi 25, 437 (1968).
[25]C. J. Delbecq, D. Schoemaker, and P. H. Yuster, Phys. Rev. B 9, 1913 (1974); 7, 3933 (1973).

[26]Y. V. G. S. Murti, G. Samuel, and S. Sivaraman, Phys. Status Solidi A 34, 615 (1976).
[27]B. Lupescu and V. Topa, Rev. Roum. Phys. 22, 503 (1977).
[28]M. Yuste and W. Bogusz, Phys. Status Solidi B 52, K133 (1972).
[29]G. Kenntner, H. J. Paus, and W. Urban, Z. Phys. B 25, 219 (1976).